Solid Freeform Fabrication of Silicon Carbide Shapes by Selective Laser Reaction Sintering (SLRS)

B.R. Birmingham and H.L. Marcus

Center for Materials Science and Engineering
The University of Texas at Austin
Austin, Texas 78712

Abstract

This paper describes an investigation of the production of silicon carbide shapes by Selective Laser Reaction Sintering (SLRS). One type of SLRS process, which combines laser sintering of silicon with acetylene decomposition, is briefly outlined, and the mechanisms important to the process are discussed. A series of test shapes are made at different acetylene pressures to determine pressure effects on conversion to silicon carbide. X-ray diffraction spectroscopy is used for bulk analysis of the shapes, and Auger electron spectroscopy is used for surface analysis. The results indicate that acetylene pressure does have a strong effect on silicon conversion to silicon carbide, and SLRS can be used successfully to make silicon carbide shapes.

Introduction

Selective Laser Reaction Sintering as a Solid Freeform Fabrication (SFF) technique and the processing equipment used for this study have been previously reported [1]. Briefly, the technique uses a scanning laser to selectively sinter a thin layer of powder. Laser sintering is accompanied by a reaction between sintering powders or sintering powder(s) and a gas precursor. The sintering/reaction combination results in a solid layer of material compositionally different from the powder source(s). Successive layers of powder are spread and selectively laser reaction sintered to build up the desired shape.

The purpose of this study is to determine if silicon carbide shapes can be made by a powder/gas precursor type SLRS process. For this study, the source powder is -325 mesh (<44mm), >99.5% purity silicon powder, and the gas precursor is high purity acetylene (C_2H_2). The basic mechanisms of the process are discussed with emphasis on possible rate limitations. A series of tests are run to determine the effect of one process variable, gas pressure, on the overall process. Results are presented and discussed.

The Silicon-Acetylene SLRS Mechanism

The proposed mechanism can be summarized as follows.

1) A scanning CO_2 laser locally heats the silicon powder bed.

2) The silicon powder is heated and melted.

3) C_2H_2 gas is adsorbed onto the liquid silicon surface where it decomposes to carbon and hydrogen.

4) Hydrogen gas desorbs as H_2.

5) Adsorbed carbon diffuses rapidly into the liquid silicon..

6) Carbon reacts with liquid silicon and solidifies as SiC.

It is important to note here that step two (2) is crucial to the success of this process. The typical material being selectively laser sintered has seconds to bond and densify. Solid state sintering mechanisms are ineffective in this time frame because solid-state diffusion effects, which are five or six orders of magnitude slower than liquid diffusion rates, are negligible [2,3]. The formation of a liquid phase, in this case liquid silicon, is critical because it can lead to solution-reprecipitation processes that are rapid enough to achieve particle bonding and densification in a SLRS time frame. A thermal model of the laser sintering system used in this study indicates surface temperatures in excess of 2000°C are readily achievable at the laser beam's focal point [4]. Silicon has a melting temperature of 1413°C. Therefore, a liquid phase can easily be created.

Thermodynamically, the decomposition of C_2H_2 and the reaction between liquid silicon and carbon to form SiC are both energetically favorable. Using 2000°C as the reaction temperature, the free energies of formation are [5];

$$C_2H_2 \Rightarrow 2C + H_2 \qquad \Delta G_f^\circ = -101{,}565 \text{ kjoules / mole}$$

$$Si_{Liquid} + C \Rightarrow \beta - SiC_{solid} \qquad \Delta G_f^\circ = -37{,}481 \text{ kjoules / mole}$$

Basic kinetic requirements of the C_2H_2 decomposition and carbon deposition steps can be established using a simple model of a laser beam moving across a surface, see

Figure 1. This model establishes a beam residence time of one second for a single pass of the laser. Scan overlap increases total beam residence time to approximately ten seconds.

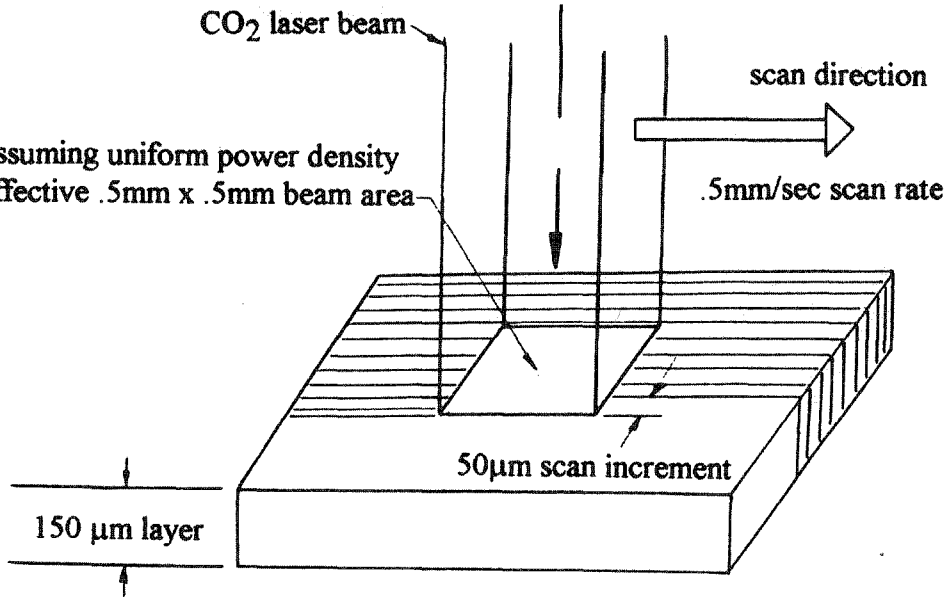

Figure 1: A simple scanning model used to determine required carbon deposition rate

Assuming a typical sintered layer thickness of 150μm and a powder porosity of 50 percent, the model indicates that a carbon deposition rate of 3μm/sec is necessary to supply the volume of silicon under the beam with enough carbon to allow full conversion to SiC. Leyendecker et al. [6] report laser induced carbon deposition rates from acetylene of 2-10μm/sec when at the temperatures and pressures used for this SLRS study, and Zong [7] reports localized rates as high as 1mm/sec. Comparing the reported rates with those required by the model, it appears that carbon deposition rate will not limit the overall process. However, it should be noted that both studies indicate that carbon deposition decreases as pressure decreases. It follows that there is some low precursor pressure below which carbon deposition rate becomes the overall rate limiting factor.

The rate that surface carbon diffuses into liquid silicon can be determined using a relationship that describes a concentration profile created by unsteady state diffusion in a single phase [8].

$$\frac{C_t - C_o}{C_s - C_o} = 1 - erf(y / \sqrt{Dt})$$

y = distance into the bulk,

C_S = surface concentration

C_o = bulk concentration at t = 0

C_t = concentration at time t

D = diffusivity of carbon in liquid silicon = 2 x 10 $^{-4}$cm^2/sec [2]

At typical SLRS scan rates and laser powers, it is reasonable to assume the material remains molten for several seconds. The above relation predicts 50 atomic percent (a/o) carbon concentration at a diffusion depth of 140μm after one second of diffusion time. Because the sintered particles have a maximum size of 44μm, it appears that carbon will diffuse rapidly enough to saturate any molten silicon present.

The silicon-carbon phase diagram [9], Figure 2, suggests behavior that will allow the final step of this process, the conversion of silicon and carbon to SiC.

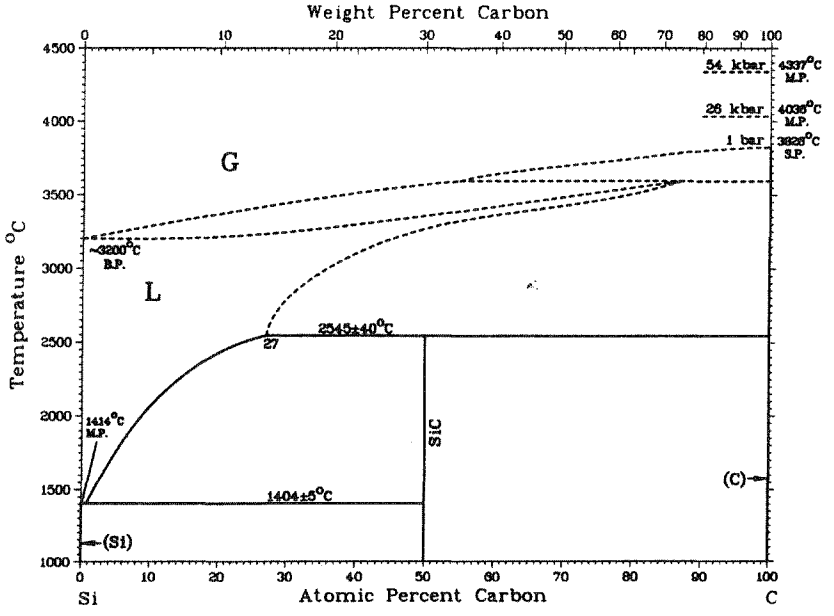

Figure 2: Silicon-Carbon binary phase diagram [9]

Above the eutectic reaction temperature at 1404 °C, carbon solubility in the liquid silicon phase dramatically increases. At 2000 °C, the Si-C phase diagram indicates a carbon solubility of approximately ten atomic percent in the liquid phase. Because of this high solubility, adsorbed carbon can diffuse into the liquid phase and react to form SiC. As predicted by the lever rule, the conversion of the saturated liquid silicon phase to SiC would continue as the liquid phase cooled. Because of scan overlap the same region will be exposed to near maximum temperatures repeatedly. Each time, some of the remaining silicon will melt and react with diffusing carbon to form more SiC. It is difficult to quantitatively predict the total amount of conversion, but amounts in excess of 50 atomic percent might be expected.

Experimental Setup

A series of single layer test coupons were produced to determine the effects of an acetylene atmosphere on the laser sintering of silicon. All operating parameters were held constant except atmosphere. The laser was scanned at 500μm/sec with a 50μm spacing between scan lines to generate a rectangular 5mm x 5mm scanned area. Each coupon area was scanned twice, using an out and back type scan, with laser power held at 1.8watts and 2.8watts, respectively. The atmosphere was provided by first evacuating the system to $<10^{-3}$ Torr and then filling with acetylene to the desired pressure. Five different pressures of acetylene were used.

Coupon 1:	700 Torr C_2H_2	(1 atmosphere = 760 Torr)
Coupon 2:	380 Torr C_2H_2	
Coupon 3:	200 Torr C_2H_2	
Coupon 4:	100 Torr C_2H_2	
Coupon 5:	50 Torr C_2H_2	

Results

X-ray diffraction spectroscopy was used for bulk phase analysis of the sintered test coupons. Figure 3 shows the diffraction pattern taken from coupon 4 .

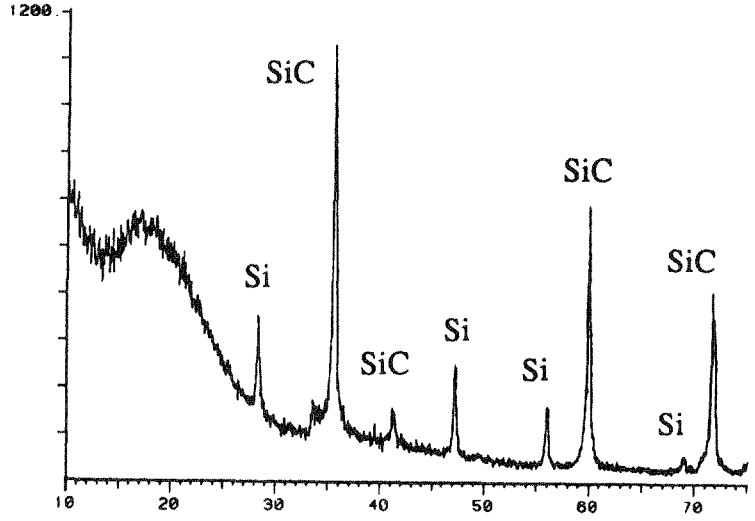

Figure 3: X-ray diffraction pattern taken of coupon 4 using $Cu_{k\alpha}$ x-rays.

Diffraction peaks for silicon and β–SiC are present. SiC conversion was semi-quantitatively determined for each coupon by comparing diffraction pattern relative peak

heights to a silicon/SiC standard run on the same x-ray equipment. Figure 4 shows a plot of SiC conversion versus pressure data obtained from the coupons.

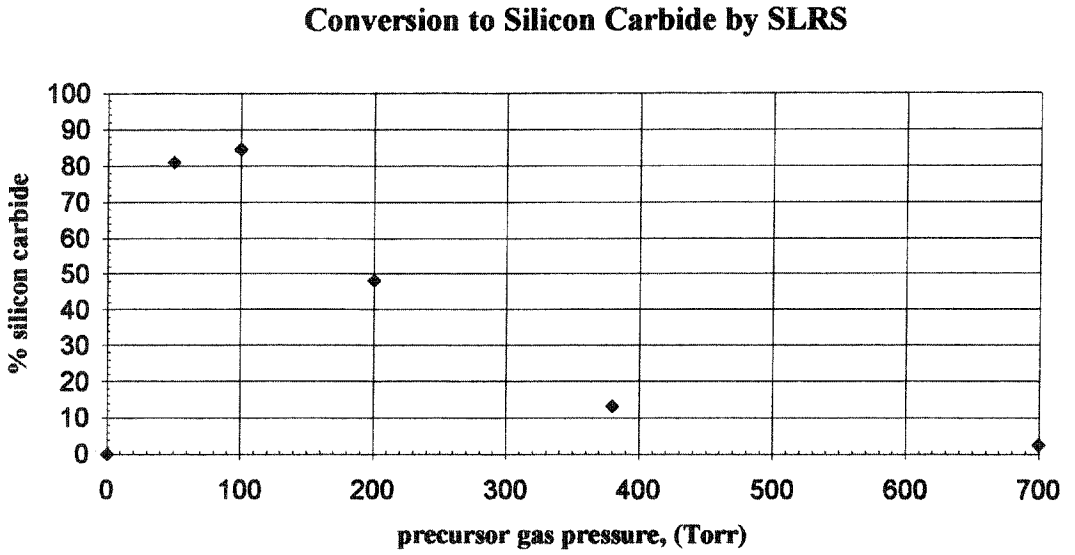

Figure 4: SiC conversion versus acetylene pressure.

Auger electron spectroscopy was used to determine the surface chemistries of the coupons. Surface spectra were taken, and then the samples were sputtered to determine concentration profiles into the bulk. Figure 5 is a plot of chemical concentration versus sputter time for coupon 4.

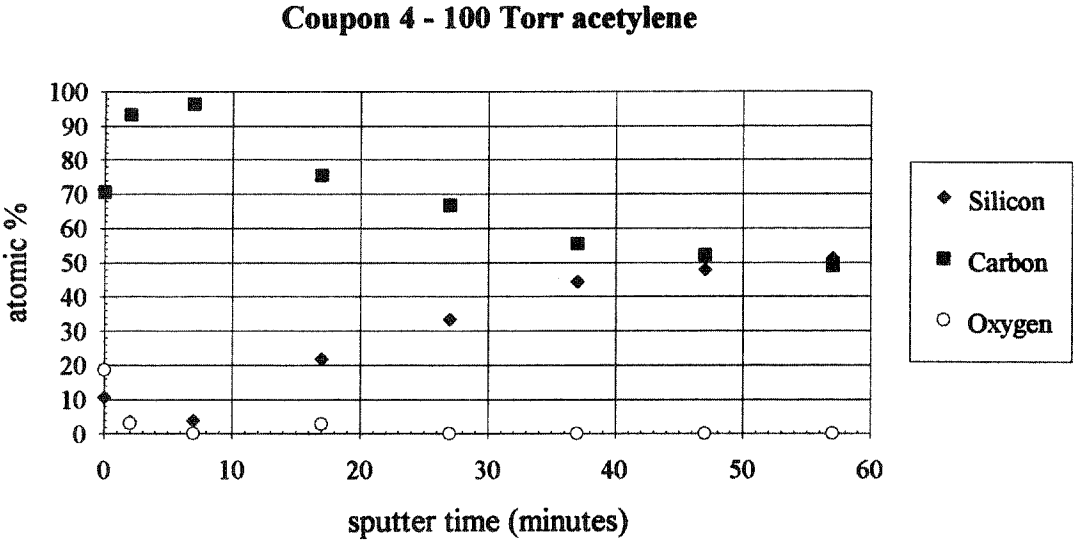

Figure 5: Chemical concentration versus sputter time for coupon 4.

The concentration profile indicates that a predominantly carbon surface gradually gives way to SiC stoichiometry. Auger peak shape and energy changes characteristic of carbon in SiC [10] were observed as stoichiometry was approached. All five coupons showed the same general behavior.

Discussion

The plot of conversion rate versus precursor pressure, Figure 4, clearly shows a maxima occurring at ~ 100 Torr C_2H_2 pressure. The decrease in conversion below this pressure can be attributed to the decrease in carbon deposition with pressure as predicted by Leyendecker et al [5]. The reduction in conversion rate as pressure increases above 100 Torr is more difficult to explain. One explanation could be that higher pressures generate initially high carbon deposition rates that cause the formation of a solid diffusion barrier at the surface of the coupons. The barrier could be SiC or carbon or a mixture of both. This barrier would then prevent further conversion of silicon to SiC by limiting the diffusion of carbon and/or silicon. The validity of this mechanism is dubious because of the lack of evidence of an increase in carbon coverage with pressure. If carbon deposition on the surface had increased with pressure as predicted, but conversion to silicon carbide was diminished because of limited diffusion, then there would have been increasing accumulations of carbon on the surfaces of the coupons. This was not detected by x-ray or Auger analysis. Another explanation focuses on a reduction in temperature at the beam focus. Initially high deposition rates might promote a surface structure with reduced infrared absorptivity and/or increased thermal conductivity. Reduced absorptivity would reduce the effective power of the laser beam. Increased thermal conductivity would increase heat flow away from the beam area. Both of these effects would lower subsequent surface temperatures, and thereby reduce carbon deposition and conversion to SiC.

Structurally, the test coupons had successfully been laser sintered to create porous 5mm x 5mm squares approximately 150μm thick. No mechanical testing was performed, but the coupons exhibited sufficient strength for handling. Figure 6, a SEM micrograph of coupon 3, reveals the carbon coated surface structures typical of all the coupons. A sputtered region of the same coupon, seen in Figure 7 reveals the underlying material. Note the crystalline structures indicative of a solution-reprecipitation process.

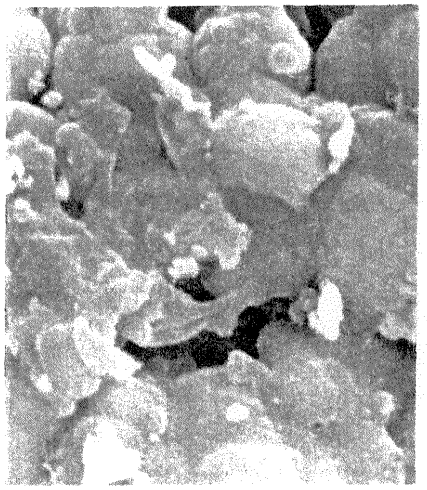

1μm

Figure 6: Surface of coupon 3

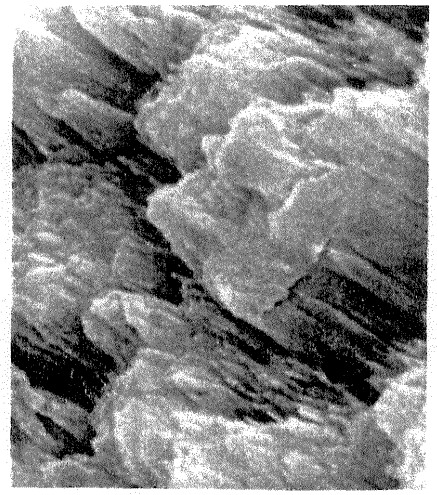

1μm

Figure 7: Underlying surface of coupon 3

As an additional test of this SLRS process, the operating parameters which yielded highest conversion to SiC in the single layer tests were used to make a multiple layer structure. The seven layer rectangular solid can be seen in Figure 8.

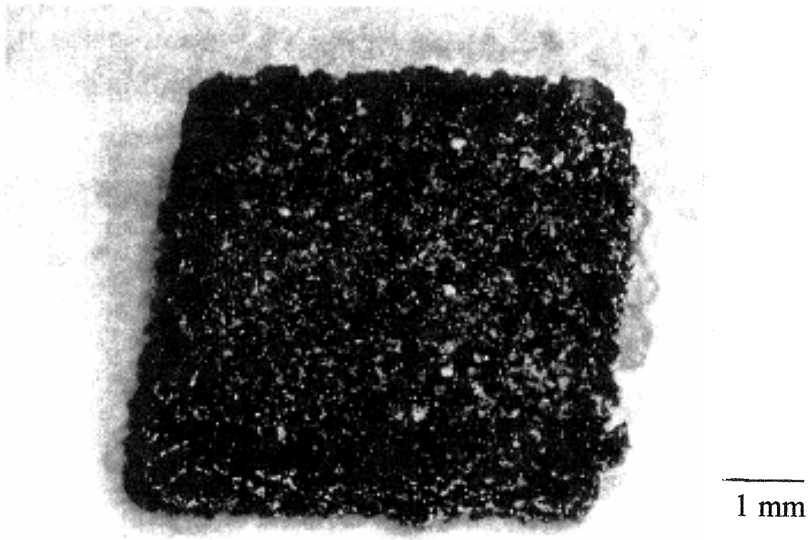

1 mm

Figure 8: 5mm x 5mm x 1mm SiC shape made by SLRS, 100 Torr C_2H_2 pressure

Conclusions

Single layer and multiple layer shapes with high SiC content were fabricated using silicon/acetylene SLRS. Precursor gas pressure was discovered to have a large but yet unexplained effect on the conversion of silicon to SiC. Work will now proceed to better

understand the mechanisms of the process so that operating parameters can be controlled to produce denser, stronger, more fully converted multiple layer SiC shapes.

Acknowledgments

Thanks go to the Office of Naval Research, grant # N00014-92-J-1514, for support of this work.

References

1. B.R. Birmingham, J.V. Tompkins, G. Zong, and H.L. Marcus, "Development of a Selective Laser Reaction Sintering Workstation," Proceedings of the Solid Freeform Fabrication Symposium, Austin, Texas, August, 1992, pp 147-153.

2. *Silicon Chemical Etching*, edited by J. Grabmier, Berlin, Springer-Verlag, 1982, p 62.

3. *Ibid*, p 28.

4. G. Zong, "Solid Freeform Fabrication Using Gas Phase Selective Area Laser Deposition," Ph.D. Dissertation, The University of Texas at Austin, Austin, Texas, 1991, pp 90-105.

5. *JANAF Thermochemical Tables*, 2nd edition, edited by D.R. Shull and H. Prophet et al., NSRDS-NBS37, U.S. Department of Commerce, National Bureau of Standards.

6. G. Leyendecker, H. Noll, D. Bauerle, P. Geittner, and H. Lydtin, "Rapid Determination of Apparent Activation Energies in Chemical Vapor Deposition," Journal of Electrochemical Society: Solid-State Science and Technology, January, 1983, pp 157-160.

7. G. Zong, "Solid Freeform Fabrication Using Gas Phase Selective Area Laser Deposition," Ph.D. Dissertation, The University of Texas at Austin, Austin, Texas, 1991, p 76.

8. F.D. Richardson, *Physical Chemistry of Melts in Metallurgy Vol.2*, London, Academic Press, 1974, pp 398-399.

9. *Binary Alloy Phase Diagrams*, 2nd edition, T.B. Massalski editor-in-chief, Ohio, ASM International, 1990, pp 882-883.

10. J.C. Riviere, *The Analyst*, **108**, 1983, p 649.